

NACA RM L55B01

MAR 30 1955

CONFIDENTIAL

7101

1

Copy
RM L55B01



RESEARCH MEMORANDUM

EFFECTS OF FREE-FLIGHT ROCKET-MODEL BOOSTER-ADAPTER
CONFIGURATIONS ON THE AERODYNAMIC CHARACTERISTICS
IN PITCH AND SIDESLIP OF A SWEEP-WING FIGHTER
AIRPLANE MODEL AT A MACH NUMBER OF 2.01

By Ross B. Robinson

Langley Aeronautical Laboratory
Langley Field, Va.

CLASSIFICATION CHANGE

To *Unclassified*
By authority *W. R. ...*
Changed by *M. Ruda* Date *2-12-71*

CLASSIFIED DOCUMENT

This material contains information affecting the National Defense of the United States within the meaning of the espionage laws, Title 18, U.S.C., Secs. 793 and 794, the transmission or revelation of which in any manner to an unauthorized person is prohibited by law.

NATIONAL ADVISORY COMMITTEE FOR AERONAUTICS

WASHINGTON

March 25, 1955

FILE COPY
To be returned to
the files of the National
Advisory Committee
for Aeronautics
Washington, D. C.

CONFIDENTIAL

NATIONAL ADVISORY COMMITTEE FOR AERONAUTICS

RESEARCH MEMORANDUM

EFFECTS OF FREE-FLIGHT ROCKET-MODEL BOOSTER-ADAPTER
CONFIGURATIONS ON THE AERODYNAMIC CHARACTERISTICS
IN PITCH AND SIDESLIP OF A SWEEP-WING FIGHTER
AIRPLANE MODEL AT A MACH NUMBER OF 2.01

By Ross B. Robinson

SUMMARY

Results are presented of a wind-tunnel investigation to determine the effects of various free-flight rocket-model booster-adapter configurations on the aerodynamic characteristics in pitch and sideslip of a swept-wing, fighter airplane model for a Mach number of 2.01. The model alone and in the presence of various booster-adapter configurations was tested through an angle-of-attack range from -2° to 11° and through a sideslip range from 0° to 13° . Normal-force, lateral-force, pitching-moment, and yawing-moment coefficients of the airplane model were measured, and schlieren photographs of the various configurations were obtained.

The results of this investigation indicate that the revised adapter configuration should substantially reduce the pitching moment of the model at separation provided the drag flap on the booster is moved rearward.

The model alone has adequate longitudinal and directional stability and should trim at a small positive angle of attack with zero incidence of the horizontal tail.

INTRODUCTION

One of the problems in the development of rocket-boosted free-flight test vehicles is to minimize the interference effects of the booster adapter on the model. The problem is complicated by mechanical requirements, which often necessitate the use of asymmetric or bluff adapter

CONFIDENTIAL

configurations. There is an analogous problem in the design of sting supports for certain supersonic wind-tunnel models where the shape of the afterbody, tail configuration, or structural details may necessitate the use of a rather bluff or asymmetrical sting support which may lead to undesirable effects.

Inasmuch as it is difficult to predict the magnitude of these interference effects, reliance must be placed on limited experiments and experience. This report presents the results of a wind-tunnel investigation of the booster-adapter interference problems of a specific free-flight rocket-model configuration. Because of the limited available aerodynamic data on this type of problem, the results of this investigation are published in the general interest to indicate the nature of the problem and the relative magnitude of the interference effects. The model involved is a swept-wing fighter-type aircraft configuration similar to a model which the Pilotless Aircraft Research Division of the Langley Laboratory used in a free-flight investigation to determine aerodynamic characteristics of the aircraft at transonic and supersonic speeds. A photograph of the model with booster is shown on the launching ramp in figure 1. The first attempt by the Langley Pilotless Aircraft Research Division to rocket-boost a free-flight model of this airplane was unsuccessful in that the model failed to follow the desired flight path after separation from the booster. Examination of the resulting telemeter records showed that the model pitched down severely immediately after separation. Analysis of the model-adapter-booster configuration indicated the possibility that the shape of the adapter might have a large effect on the flow over the horizontal tail. Accordingly, a revised booster adapter was designed.

The present tunnel investigation was then made in the Langley 4- by 4-foot supersonic pressure tunnel to determine the effects of the original and revised booster-adapter configurations on the aerodynamic characteristics of the model at a Mach number of 2.01. Force and moment data and schlieren photographs were obtained for the model in the presence of the booster adapter and for the model alone through an angle-of-attack range from about -2° to about 11° and through an angle-of-sideslip range from 0° to about 13° . After the wind-tunnel tests, a flight of the model with the revised booster configuration was made by the Langley Pilotless Aircraft Research Division and the flight was successful.

COEFFICIENTS AND SYMBOLS

The results of this investigation are presented as standard NACA coefficients of forces and moments. The data are referred to the body-axes system with the reference center of moments at 42 percent of the wing mean geometric chord and 25 percent of the mean geometric chord

above the horizontal reference line through the fuselage nose. The coefficients and symbols are defined as follows:

C_N	normal-force coefficient, $\frac{\text{Normal force}}{qS}$
C_Y	lateral-force coefficient, $\frac{\text{Lateral force}}{qS}$
C_m	pitching-moment coefficient, $\frac{\text{Pitching moment}}{qS\bar{c}}$
C_n	yawing-moment coefficient, $\frac{\text{Yawing moment}}{qSb}$
ΔC_N	incremental normal-force coefficient due to addition of adapter
ΔC_m	incremental pitching-moment coefficient due to addition of adapter
$(\Delta C_Y)_t$	incremental lateral-force coefficient due to addition of horizontal and vertical tails
$(\Delta C_n)_t$	incremental yawing-moment coefficient due to addition of horizontal and vertical tails
q	free-stream dynamic pressure
S	area of theoretical wing, including body intercept (see fig. 2)
b	wing span
c	local wing chord
\bar{c}	wing geometric chord, $\frac{2}{S} \int_0^{b/2} c^2 dy$
α	angle of attack of wing, deg
β	angle of sideslip of fuselage reference line, deg
i_t	angle of incidence of horizontal tail, deg

MODEL AND APPARATUS

A three-view drawing of the model is presented in figure 2. Details of the original and revised booster adapters and a sketch of the various model-booster-adapter combinations are shown in figure 3. Photographs of the various configurations are shown in figure 4. Geometric characteristics of the model are presented in table I.

The model had a wing with 35° sweep of the 29.88 percent chord line, an aspect ratio of 4.50, a taper ratio of 0.28, and NACA 65A007 and NACA 65A006 airfoil sections at the root and tip, respectively. The wing had zero twist and dihedral and 1° incidence with respect to the fuselage reference line. The horizontal- and vertical-tail assembly was removable as a unit for investigation of the wing-body combination. There were no movable control surfaces; the horizontal tail was fixed at 0° deflection.

Three configurations of adapters were investigated (see figs. 3 and 4): (1) the original design, (2) a revised version designed to reduce the negative pitching-moment increment induced by the adapter, and (3) the revised adapter with a drag flap opened 60° to facilitate booster breakaway.

Force and moment measurements for the airplane only were made in the presence of the booster-adapter combination by means of a four-component strain-gage balance. Drag and rolling-moment coefficients were not measured. The booster and adapter contained no instrumentation. Schlieren photographs of all configurations were made. The model, booster, adapters, balance, and sting were supplied by the contractor.

TEST CONDITIONS

The conditions for the tests were as follows:

Mach number	2.01
Reynolds number, based on \bar{c}	0.55×10^6
Stagnation pressure, lb/sq in. abs	13
Stagnation temperature, $^\circ\text{F}$	100
Stagnation dewpoint, $^\circ\text{F}$	-25
Mach number variation	± 0.015
Flow-angle variation in horizontal or vertical plane, deg . . .	± 0.1

CORRECTIONS AND ACCURACY

The angles of attack and sideslip were corrected for the deflection of the balance and sting under load. No corrections were applied to the data to account for the tunnel-flow variations.

The estimated errors in the data are as follows:

C_N	± 0.003
C_Y	± 0.003
C_m	± 0.002
C_n	± 0.0005
α , deg	± 0.1
β , deg	± 0.1

RESULTS AND DISCUSSION

The aerodynamic characteristics in pitch and in sideslip for the various configurations are presented in figures 5 to 11 and schlieren photographs are presented in figure 12.

Effects of Adapter Shape

At small angles of attack the revised adapter induced about half as much incremental pitching-moment coefficient as did the original configuration (figs. 5 and 7). As a result, the model should have only a small initial pitching moment if separation from the adapter-booster combination occurs at an angle of attack near 0° . However, with the drag flap on the revised adapter open, the model would have a large negative pitching moment. Hence, consideration should be given to moving the drag flap rearward. A comparison of the complete-model results (figs. 5 and 7) with those for the model with the tail removed (figs. 6 and 7) indicates that the incremental pitching moments and normal forces caused by the adapters result primarily from the effects of altered flow over the horizontal tail rather than from flow changes on the wing-body combination. An indication of the extent of the flow changes over the rear of the model produced by the adapters may be obtained by comparing schlieren photographs of the model alone (fig. 12(a) and fig. 12(b)) with those of the model with the various adapter configurations (figs. 12(c), 12(d), and 12(e)). The flow over the entire tail assembly is altered when the flap is extended.

Although the effects of the revised adapter on the aerodynamic characteristics of the model are erratic, a substantial reduction in the directional stability of the airplane is indicated for both the flap-retracted and flap-extended configurations (fig. 8). Both adapters produce areas of disturbed flow in the region of the vertical tail (figs. 12(d) and 12(e)). If booster separation occurs near zero sideslip, the model should have no significant initial yawing moment.

A subsequent launching by the Langley Pilotless Aircraft Research Division of a free-flight model of the configuration equipped with the revised booster adapter and a more rearward drag flap essentially verifies the wind-tunnel results in that the model was successfully separated from the booster.

Aerodynamic Characteristics of the Model Alone

The results for the model alone indicate adequate longitudinal stability for a center-of-gravity location at 44 percent of the mean geometric chord and 25 percent of the mean geometric chord above the horizontal reference line (fig. 9). A trim angle of attack of about 3.4° is indicated for $i_t = 0^\circ$ (fig. 9) with a resulting C_N of about 0.19.

The wing-body combination was, of course, directionally unstable (fig. 10), but the addition of the tail provides a large stabilizing yawing moment (figs. 10 and 11); as a result, the complete model at $\alpha = -2.2^\circ$ has ample directional stability. From the magnitude of the directional stability, it might be expected that the airplane would have adequate stability to moderate positive angle of attack notwithstanding the rearward location of the center of gravity.

CONCLUDING REMARKS

The results of this investigation indicate that the revised adapter configuration should substantially reduce the pitching moment of the model at separation provided the drag flap on the booster is moved rearward.

The model alone has adequate longitudinal and directional stability and should trim at a small positive angle of attack with zero incidence of the horizontal tail.

Langley Aeronautical Laboratory,
National Advisory Committee for Aeronautics,
Langley Field, Va., January 17, 1955.

TABLE I.- DIMENSIONS OF MODEL

Wing:

Root airfoil section	NACA 65A007
Tip airfoil section	NACA 65A006
Total area (theoretical), sq ft	0.1135
Span, in.	8.572
Mean geometric chord, in.	2.107
Root chord, in.	2.970
Tip chord, in.	0.845
Taper ratio, in.	0.284
Aspect ratio	4.50
Sweep, 0.2988 chord line, deg	35
Incidence at fuselage center line, deg	1
Dihedral, deg	0
Geometric twist, deg	0
Length of fence, in.	1.18
Spanwise location of fence, in.	2.91

Horizontal Tail:

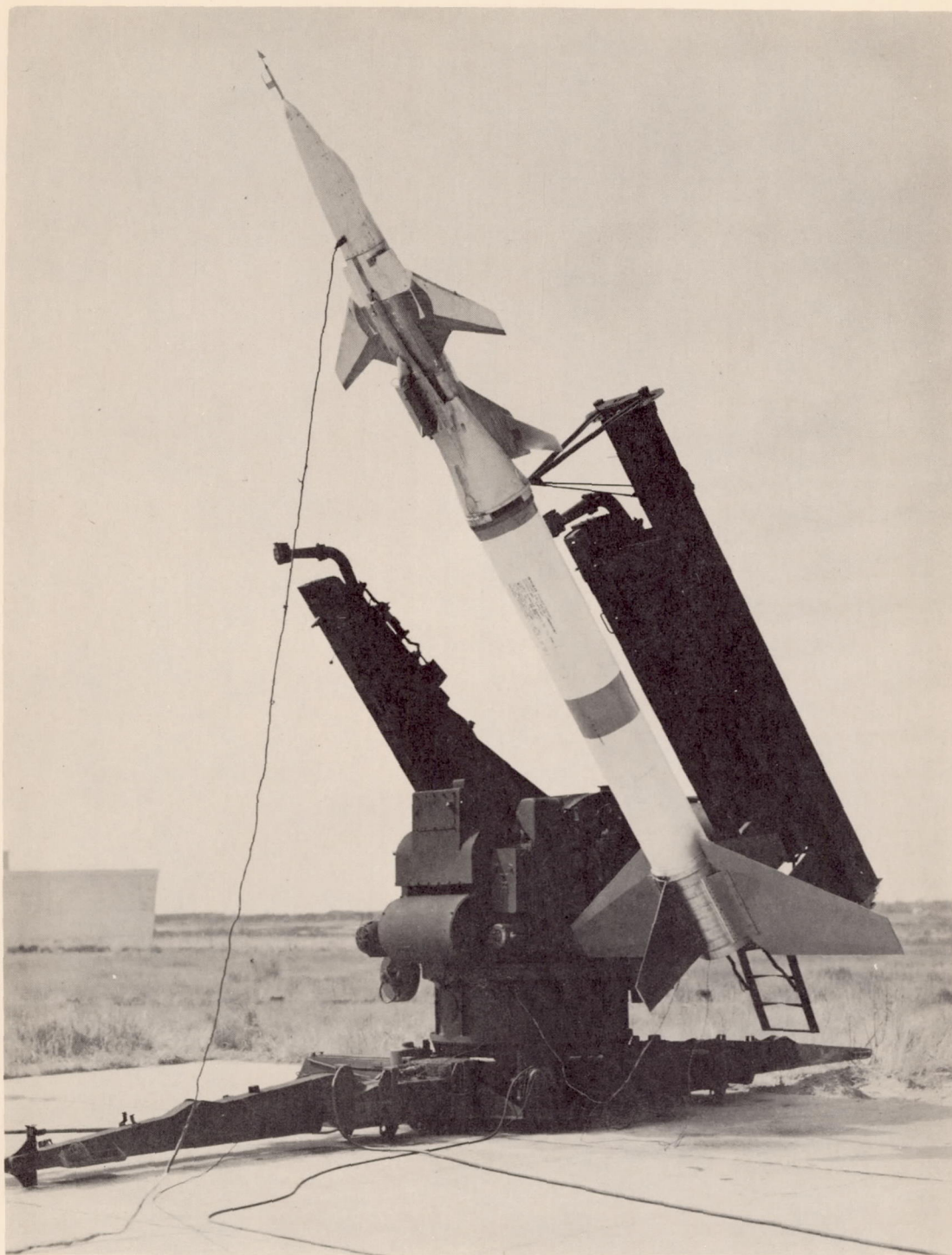
Root airfoil section normal to 0.293 chord	NACA 65A007
Tip airfoil section normal to 0.293 chord	NACA 65A007
Area including fuselage, sq ft	0.0243
Span, in.	3.40
Mean geometric chord, in.	1.078
Root chord, parallel to plane of symmetry, in.	1.413
Tip chord, in.	0.648
Taper ratio	0.458
Aspect ratio	3.3
Sweep of 0.2934 chord, deg	35
Dihedral, deg	10

Vertical Tail:

Airfoil section parallel to fuselage center line	NACA 65A007
Area (theoretical), sq ft	0.03118
Span, in.	1.980
Root chord, in.	3.240
Tip chord, in.	1.296
Sweep of 0.25 chord, deg	45
Taper ratio	0.40
Aspect ratio	0.873

Fuselage:

Length, in.	14.47
Maximum fuselage depth, in.	1.43
Length/depth ratio	10.11



L-83989

Figure 1.- Langley Pilotless Aircraft Research Division free-flight model with original booster-adapter configuration.

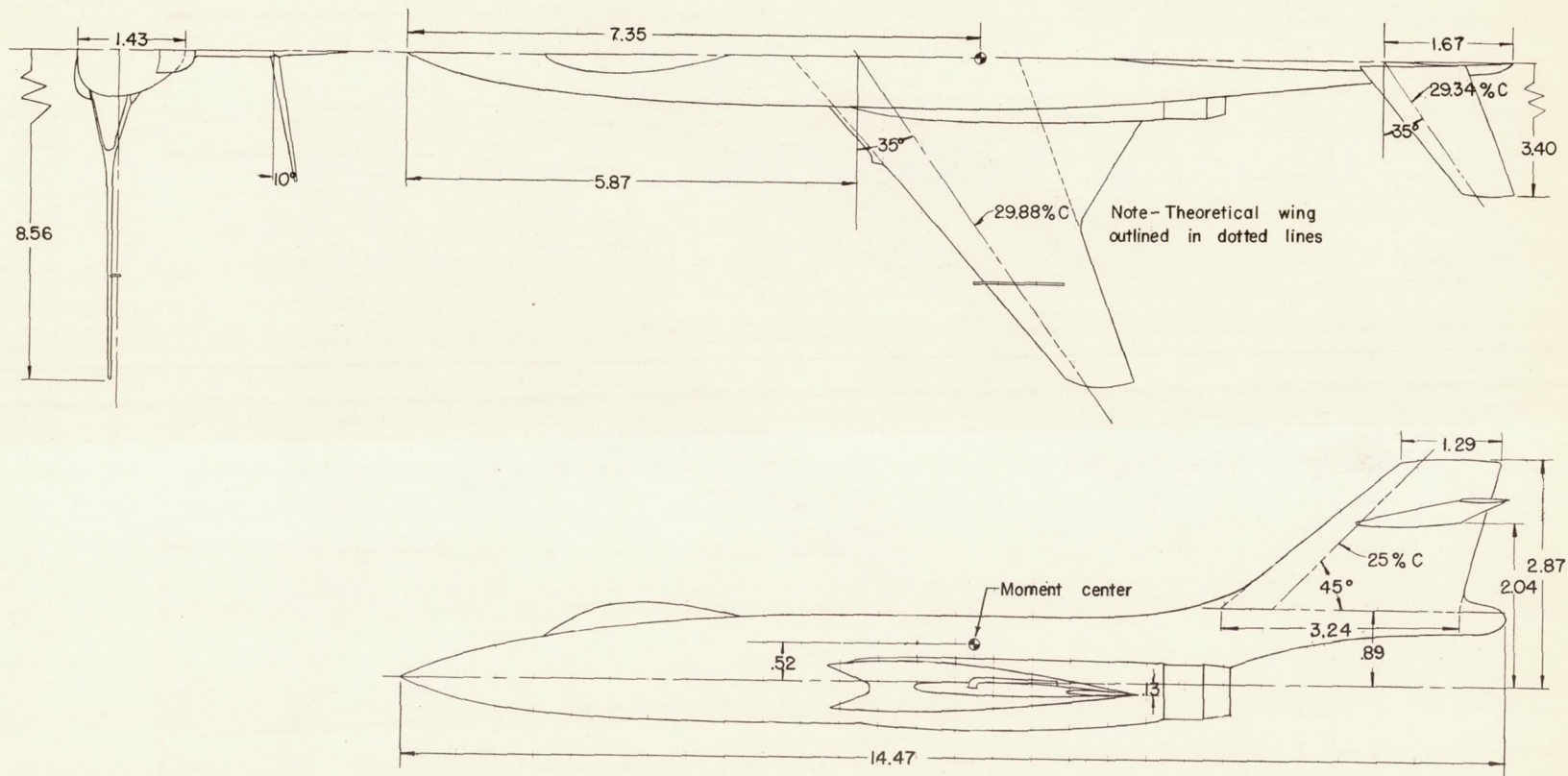
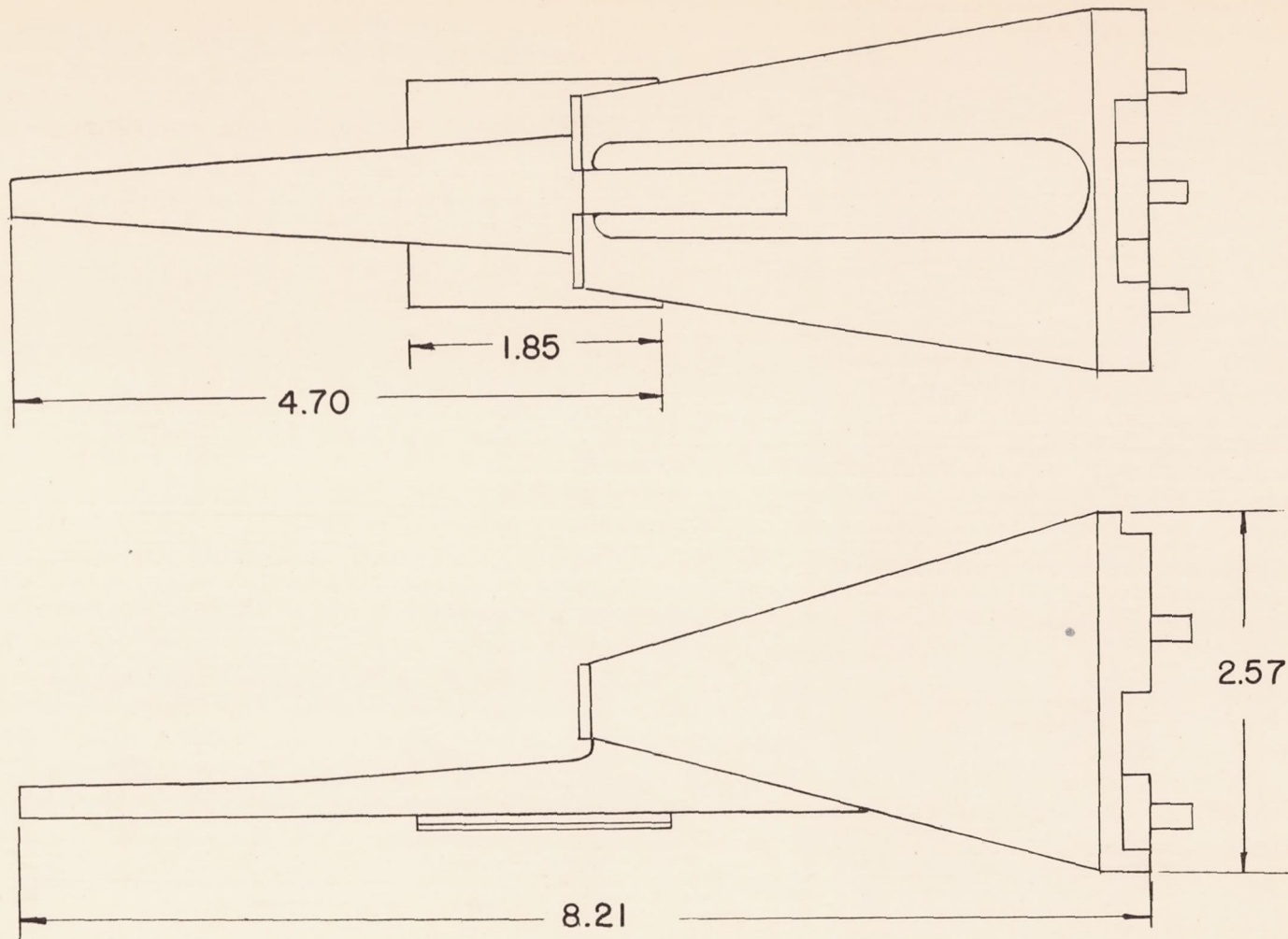
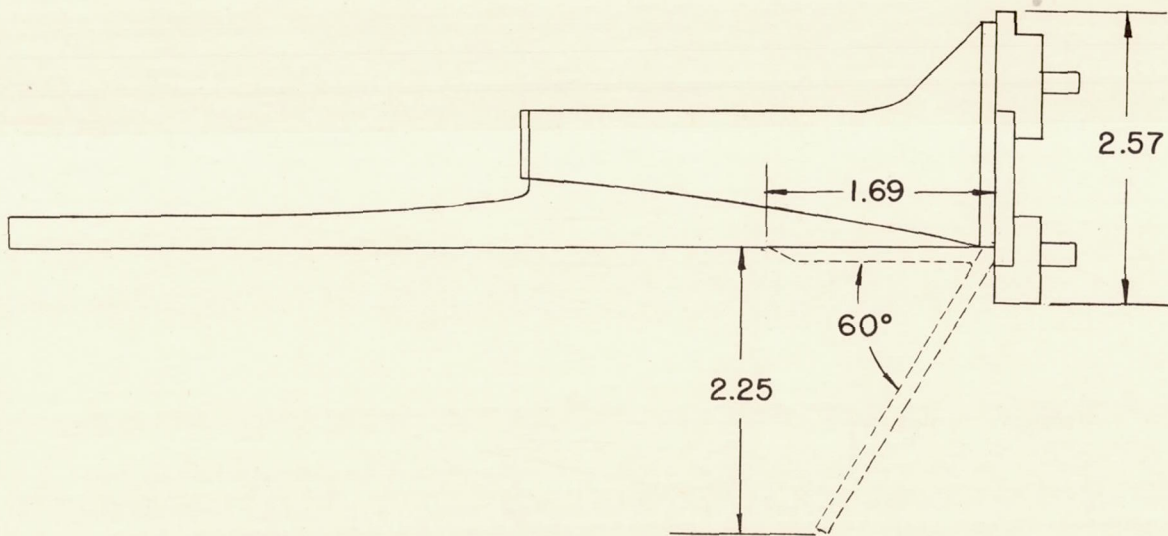
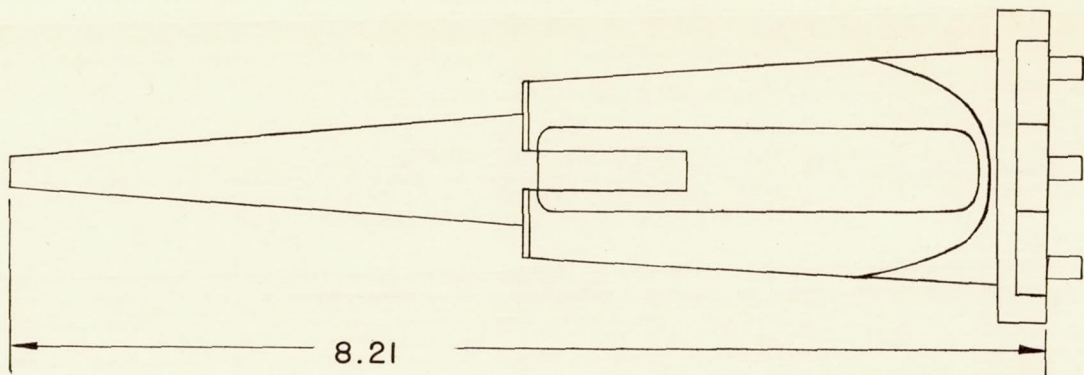


Figure 2.- Three-view drawing of model. All dimensions are in inches.



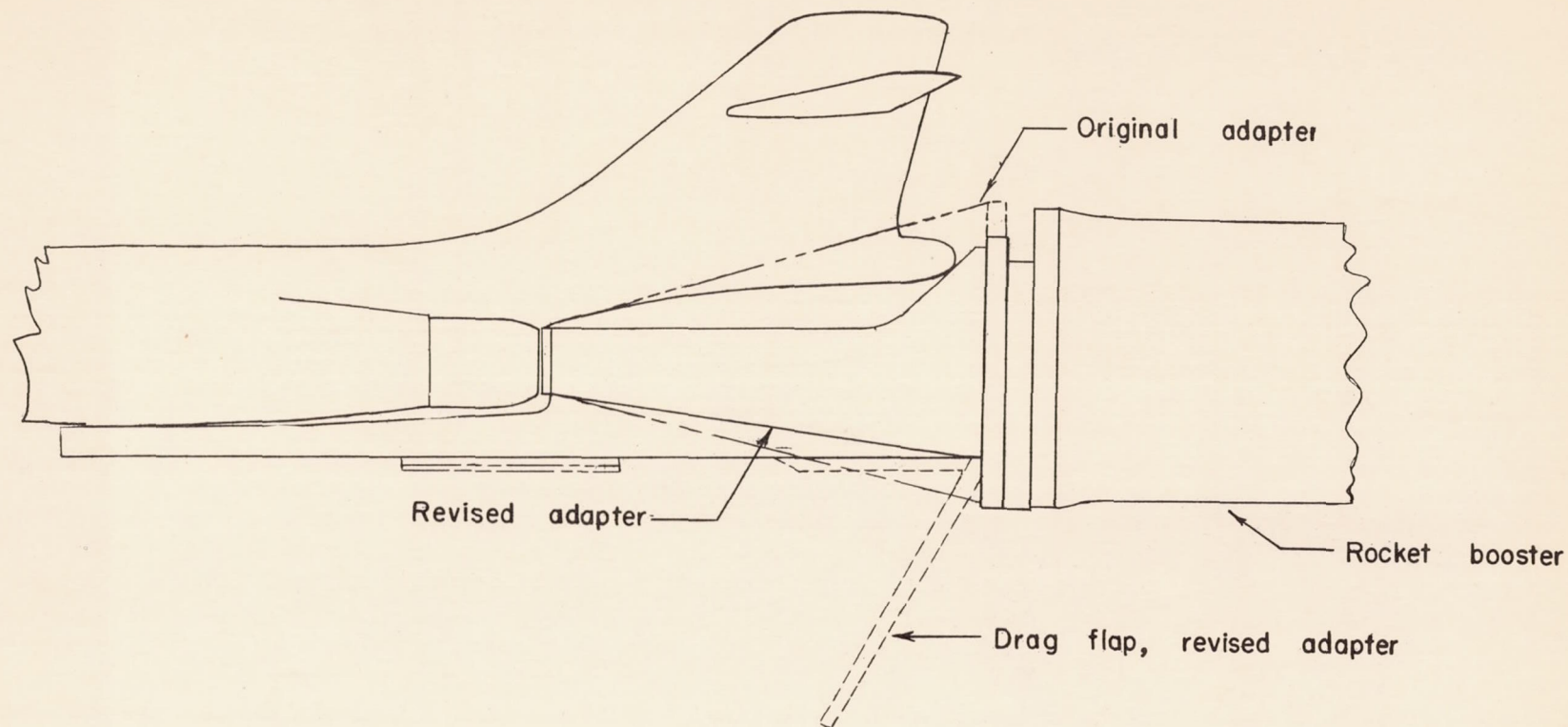
(a) Original configuration.

Figure 3.- Booster-adaptor configurations. All dimensions are in inches unless otherwise noted.



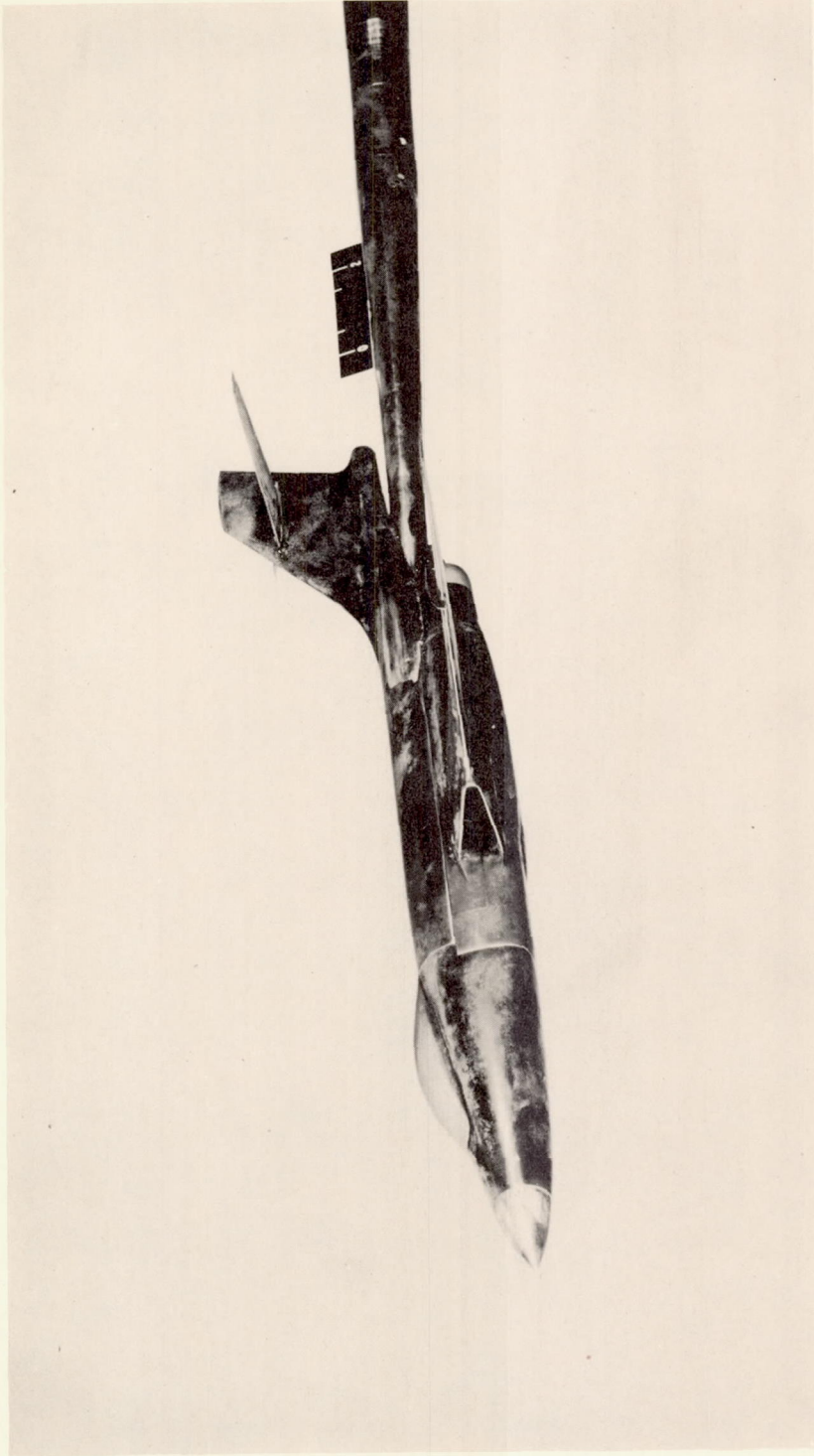
(b) Revised configuration and flap.

Figure 3.- Continued.



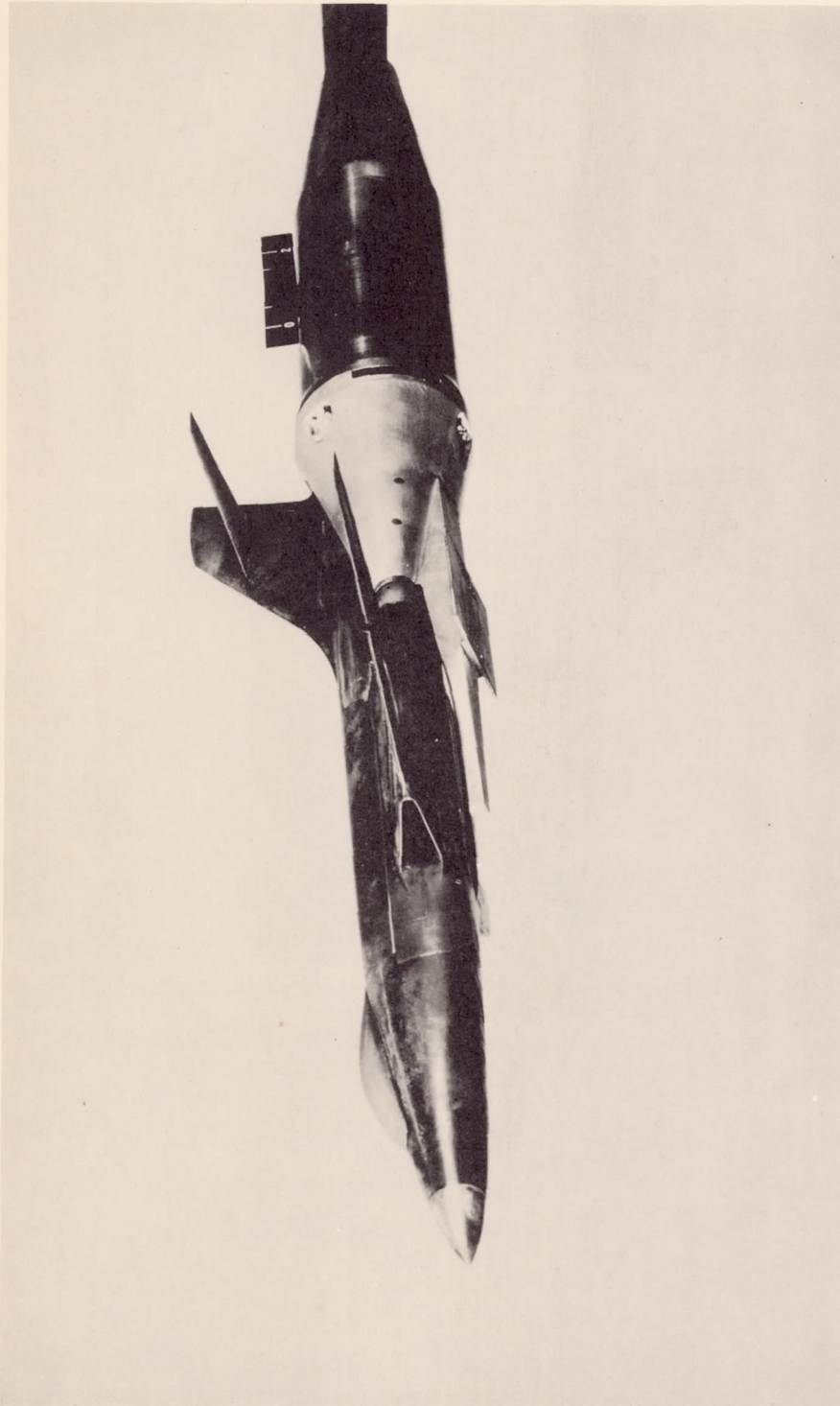
(c) Composite of various configurations.

Figure 3.- Concluded.



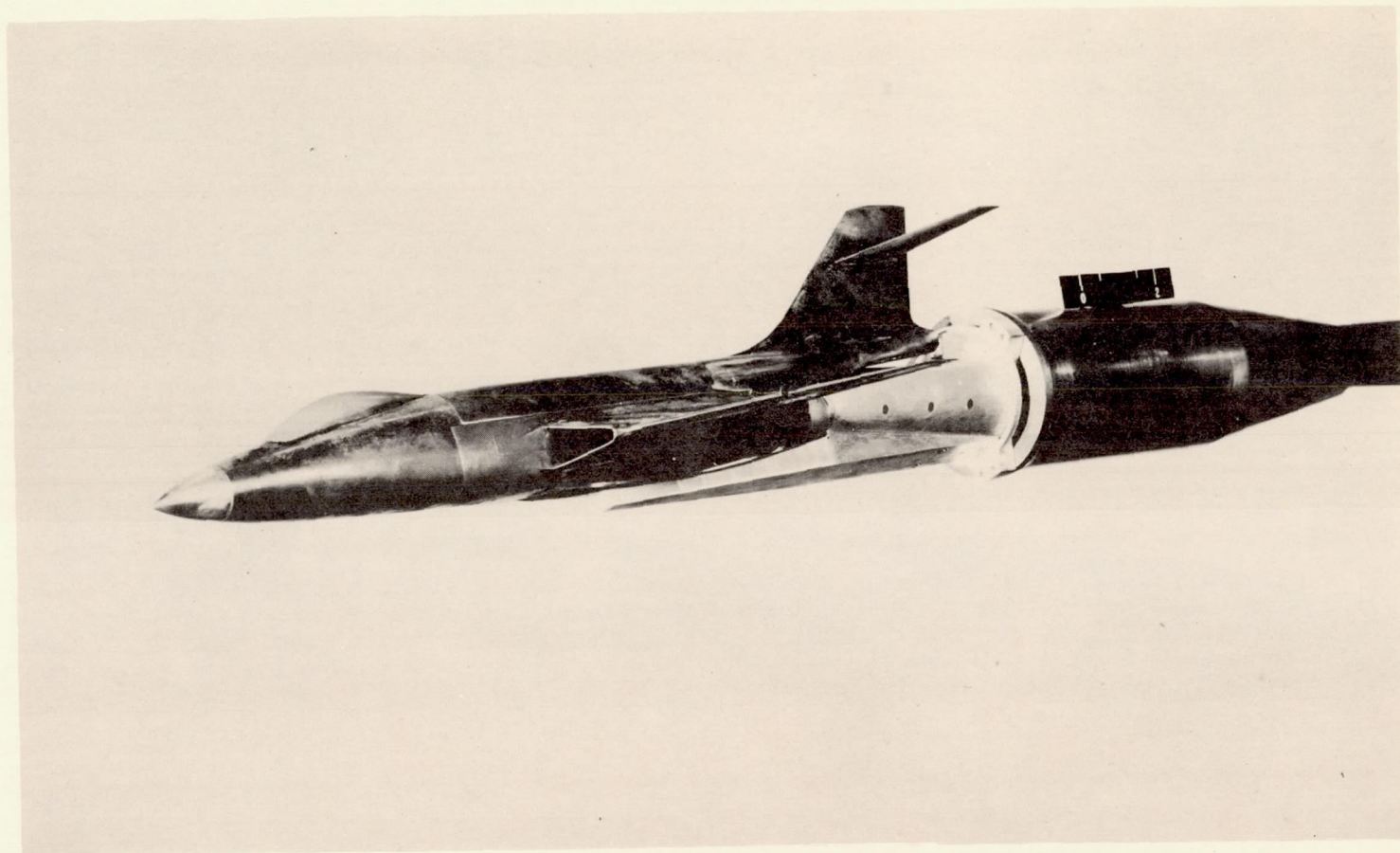
(a) Complete model alone. L-86129

Figure 4.- Photographs of the various configurations.



(b) Complete model; original adapter. L-86128

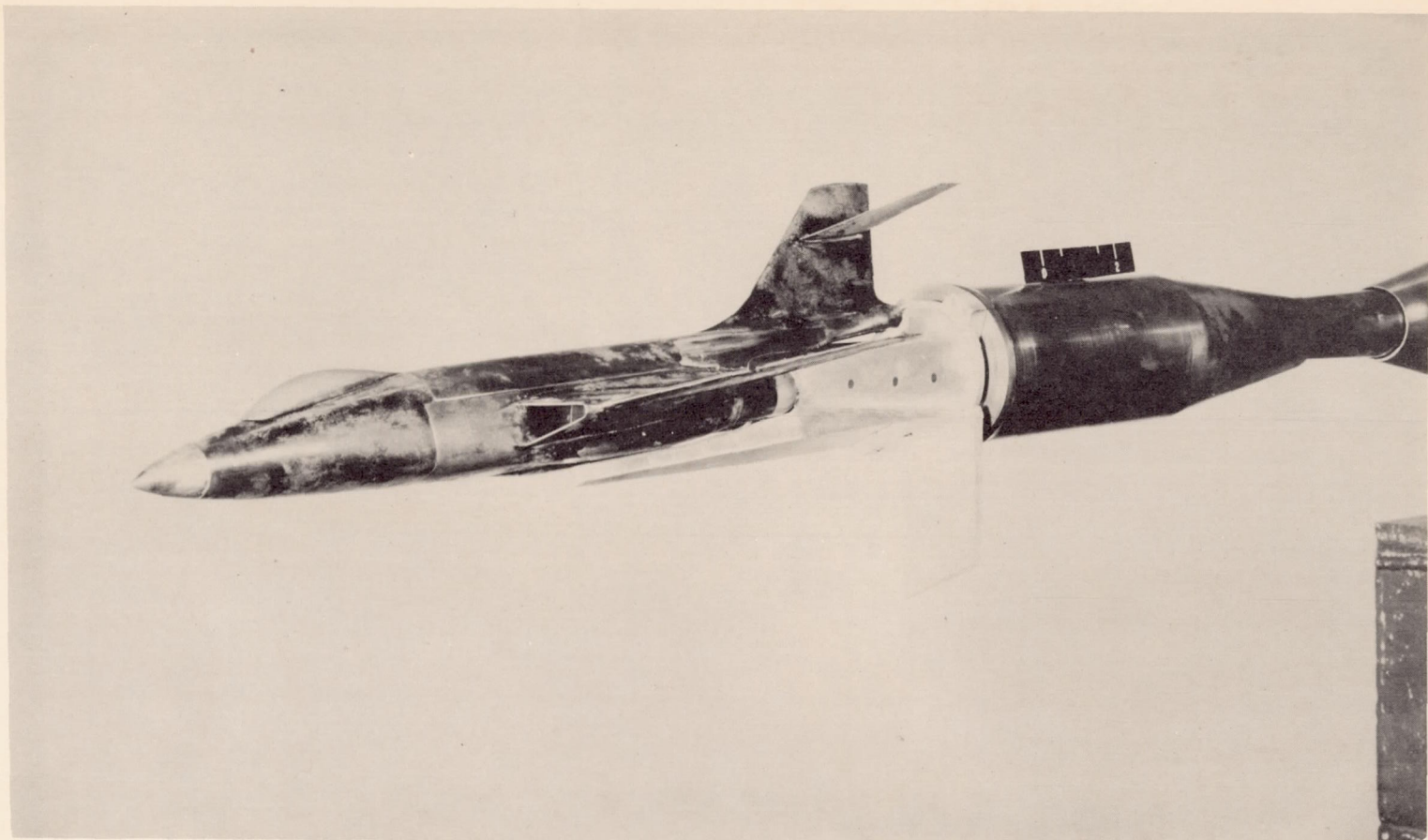
Figure 4.- Continued.



(c) Complete model; revised adapter.

L-86127

Figure 4.- Continued.



L-86126
(d) Complete model; revised adapter with drag flap extended.

Figure 4.- Concluded.

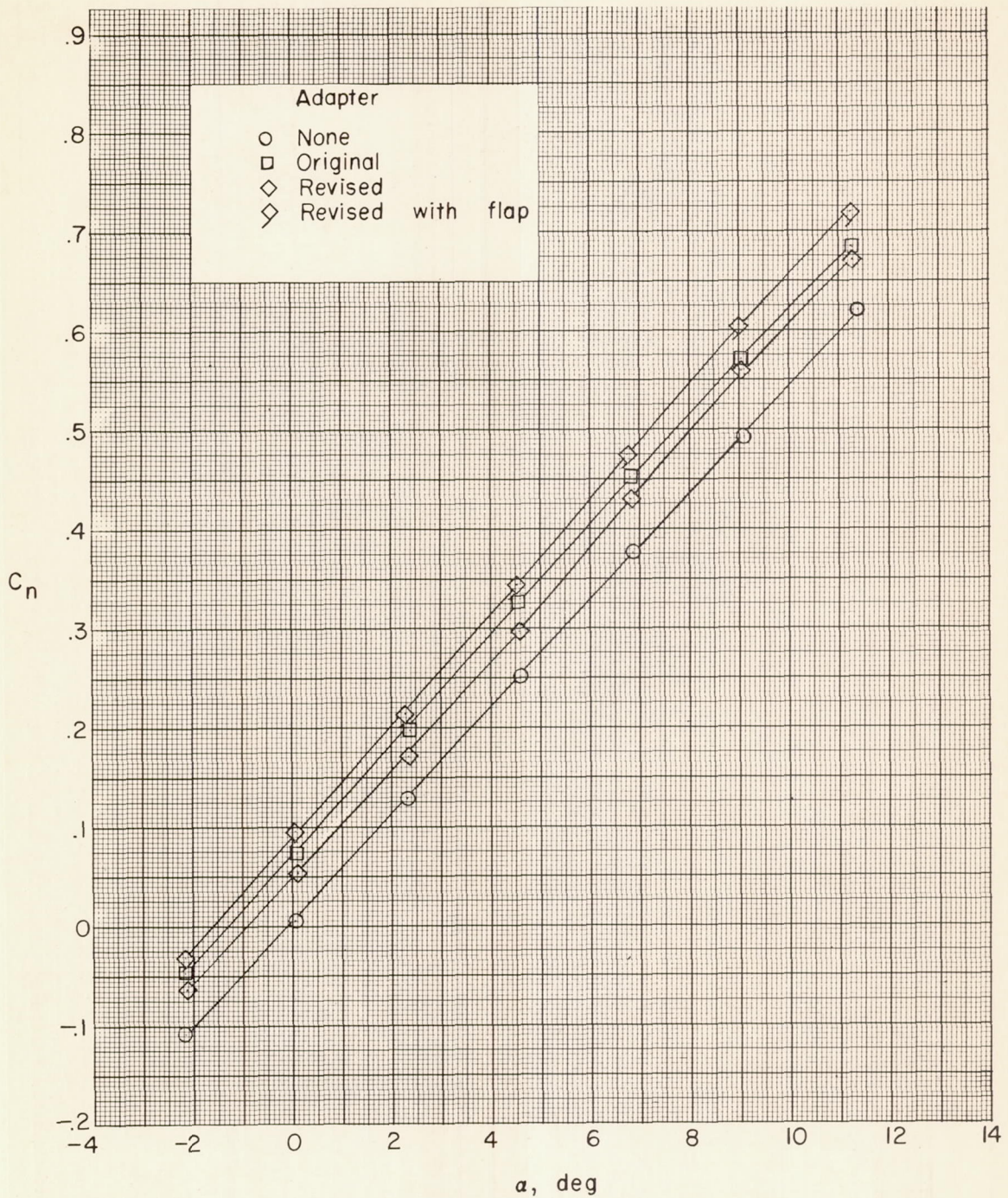


Figure 5.- Effects of various adapters on the aerodynamic characteristics in pitch of the complete model. $\beta = 0.3^\circ$.

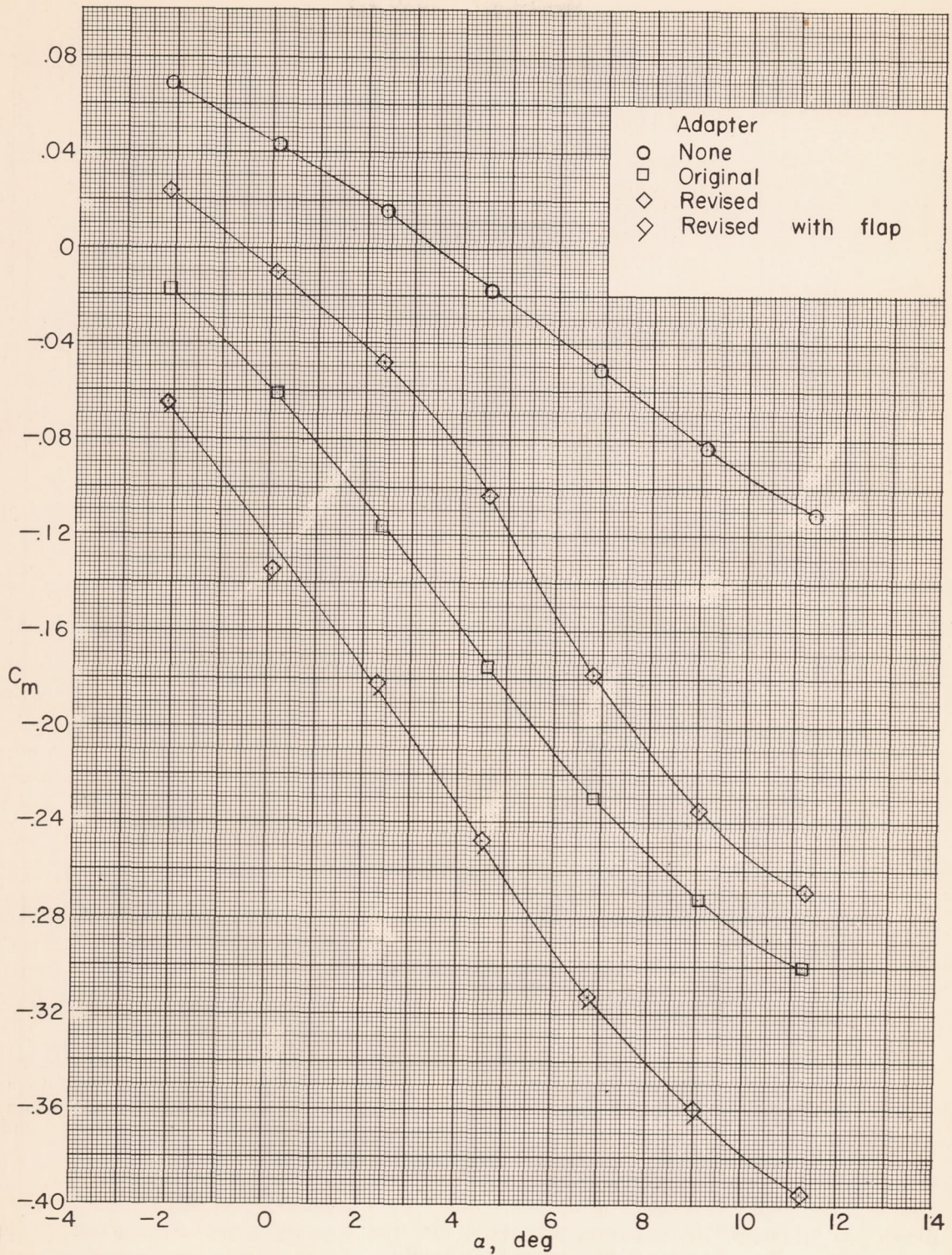


Figure 5.- Concluded.

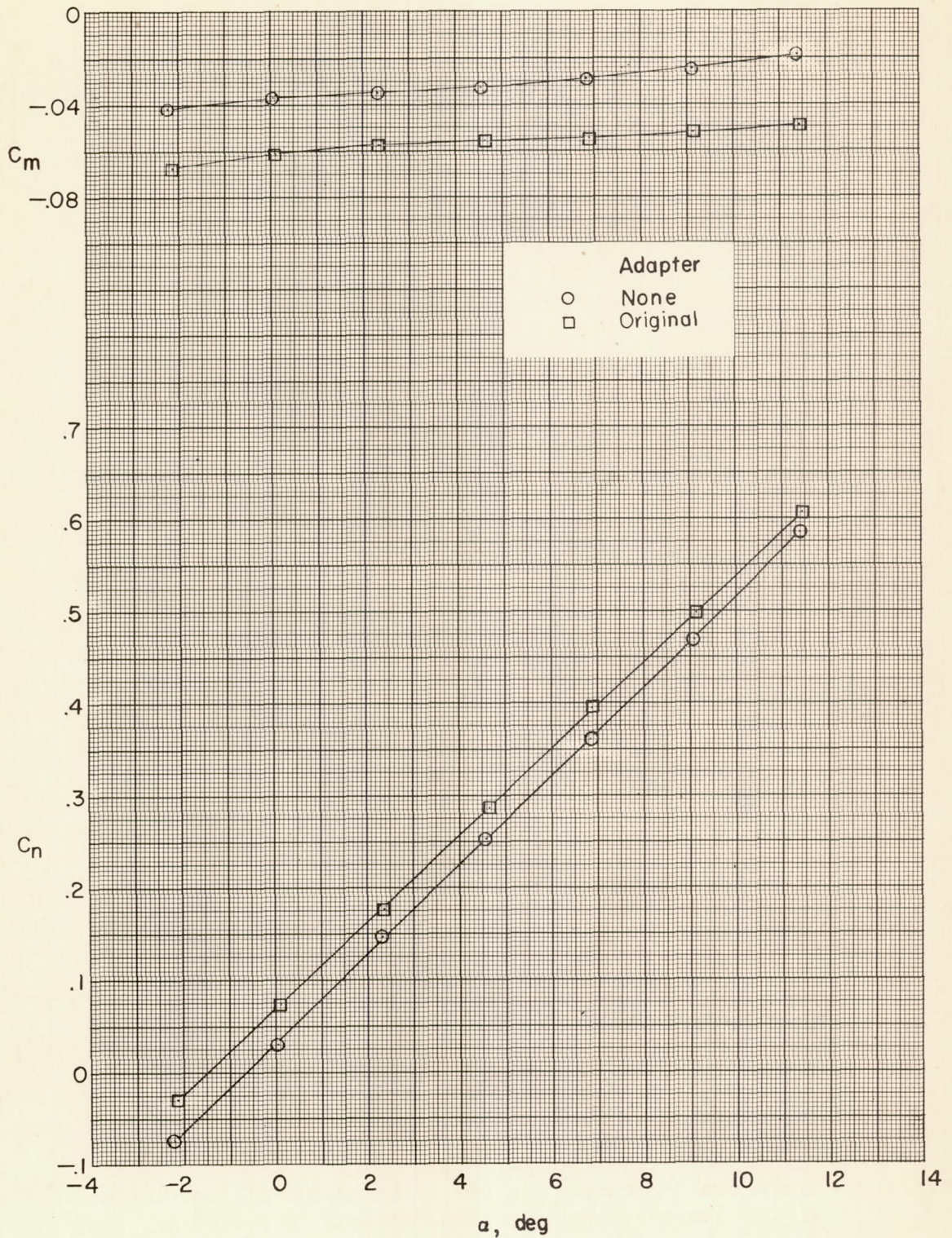


Figure 6.- Effects of original adapter on the aerodynamic characteristics in pitch of the wing-fuselage combination. $\beta = 0.3^\circ$.

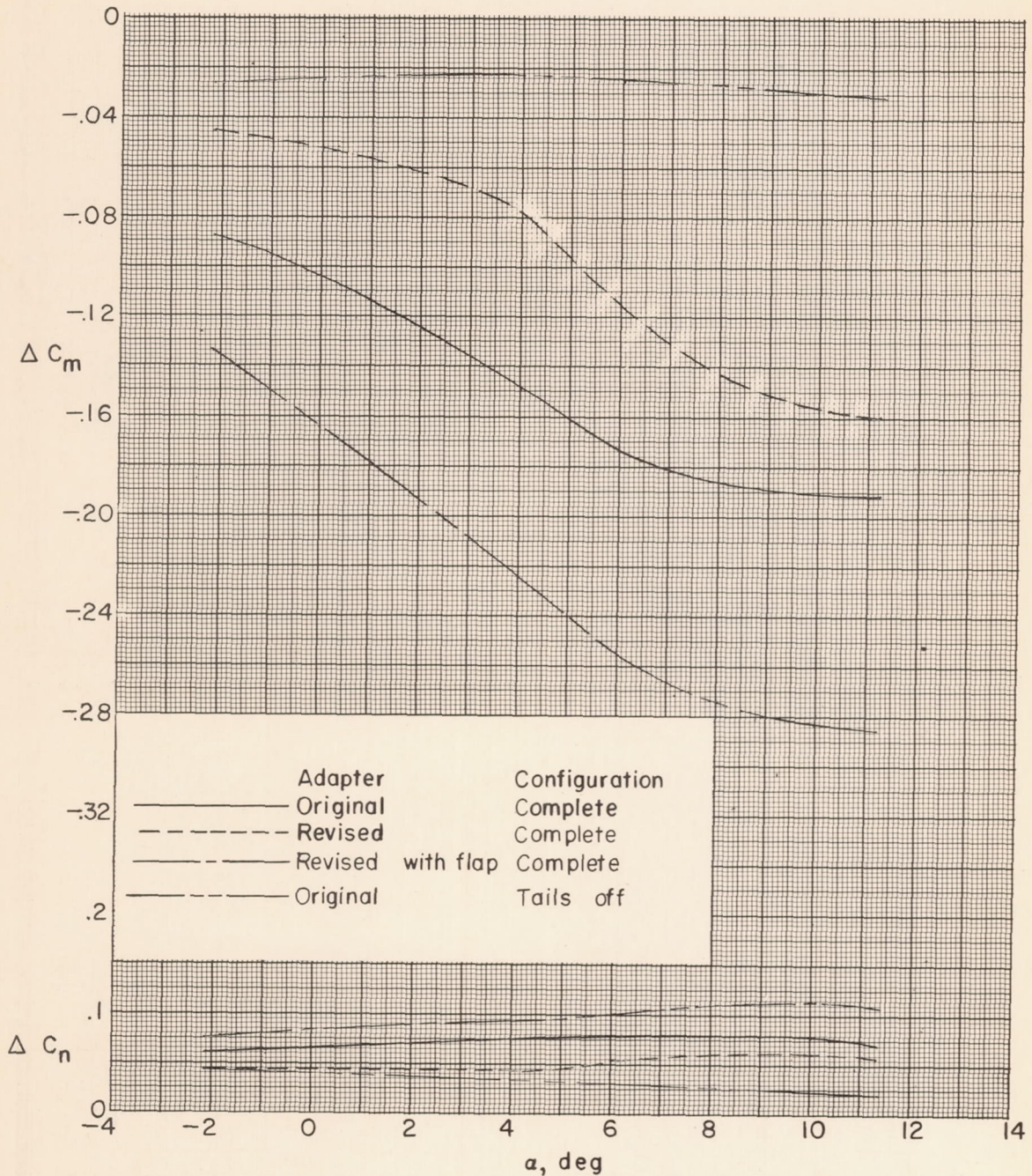


Figure 7.- Incremental normal-force and pitching-moment coefficients due to the various adapter configurations. $\beta = 0.3^\circ$.

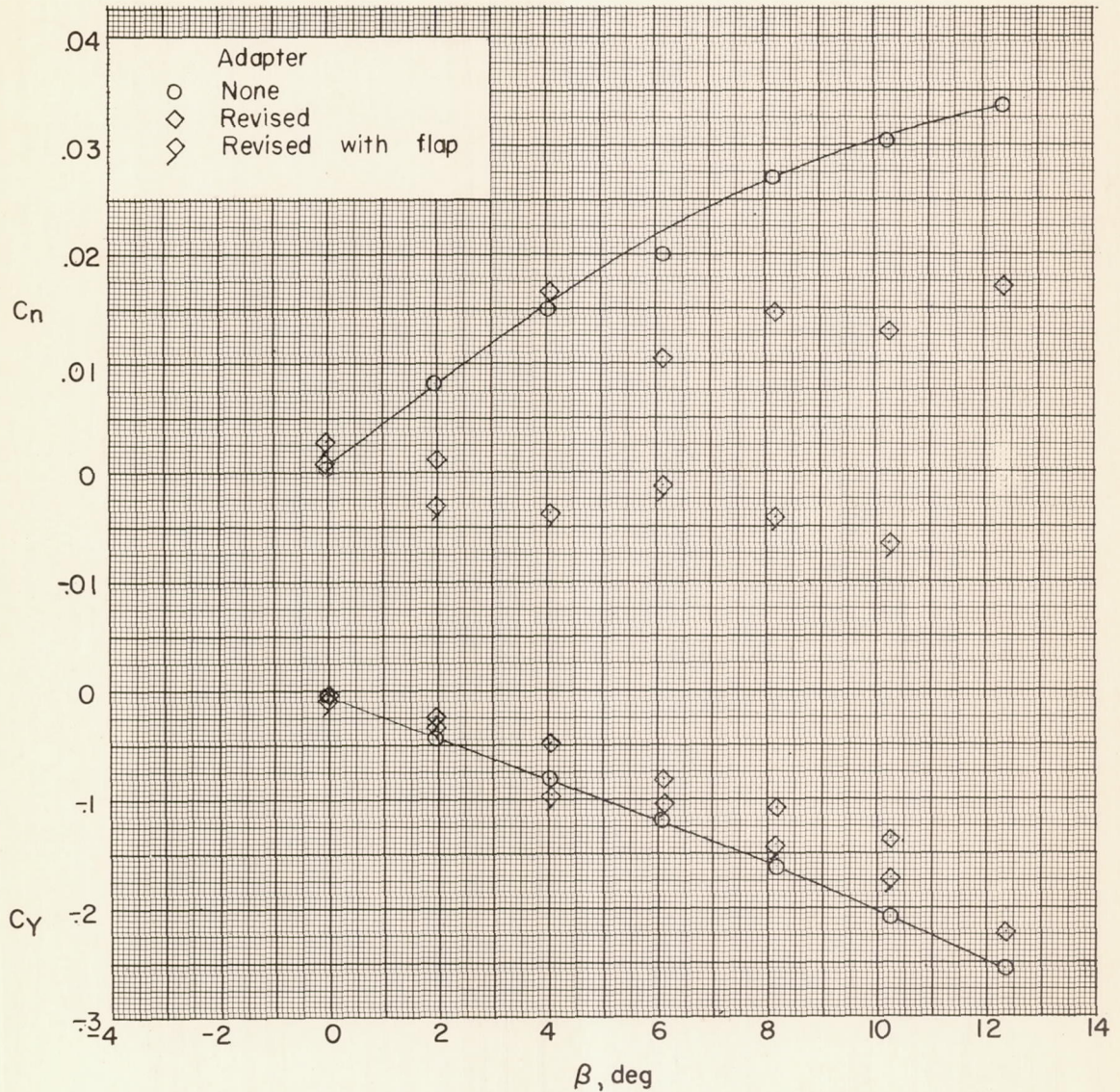


Figure 8.- Effects of the revised adapter, with and without flaps, on the aerodynamic characteristics in sideslip of the complete model. $\alpha = -2.2^\circ$.

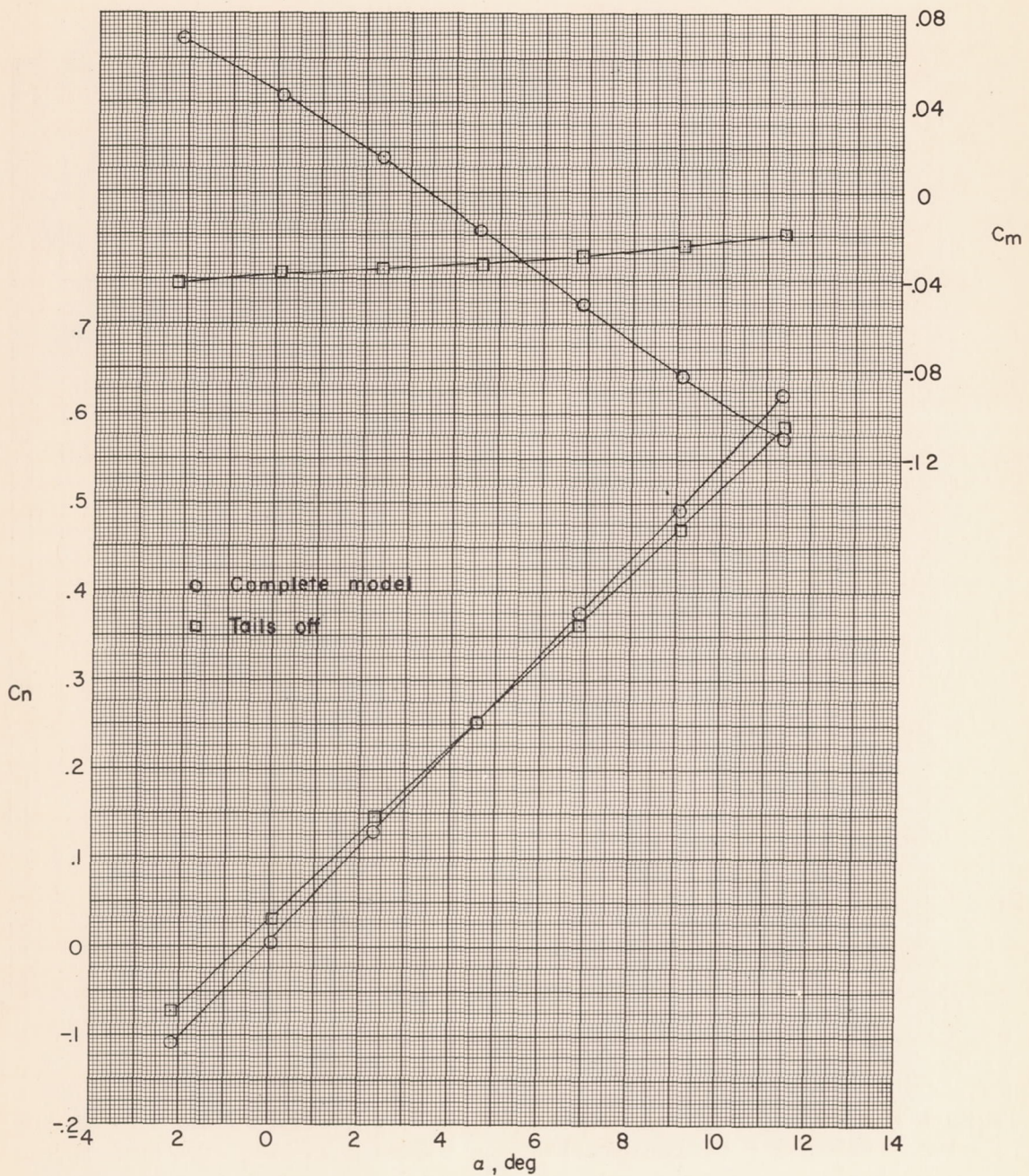


Figure 9.- Effect of horizontal and vertical tails on the aerodynamic characteristics in pitch. $\beta = 0.3^\circ$; $i_t = 0^\circ$; booster adapter off.

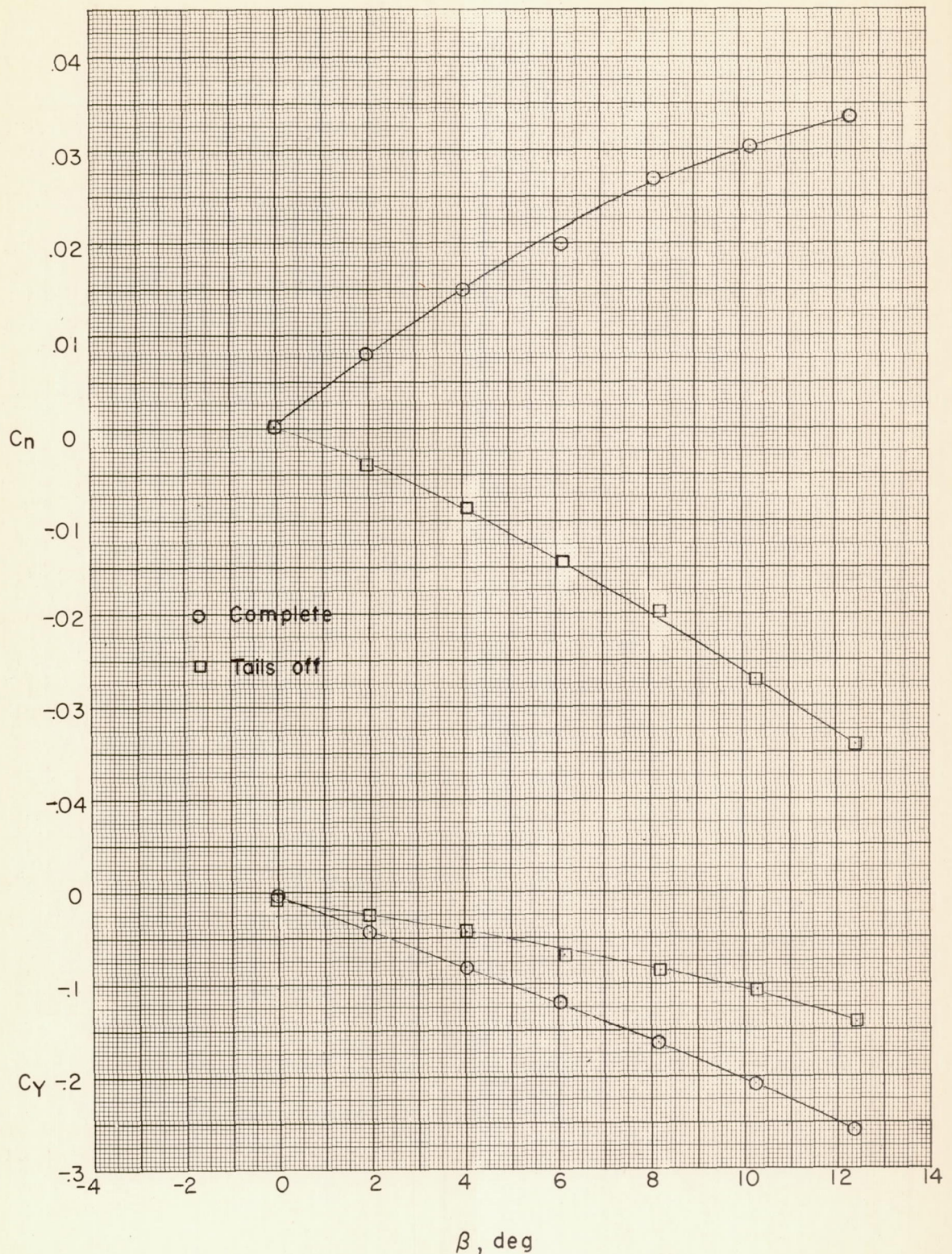


Figure 10.- Effect of horizontal and vertical tails on the aerodynamic characteristics in sideslip. $\alpha = -2.2^\circ$; booster adapter off.

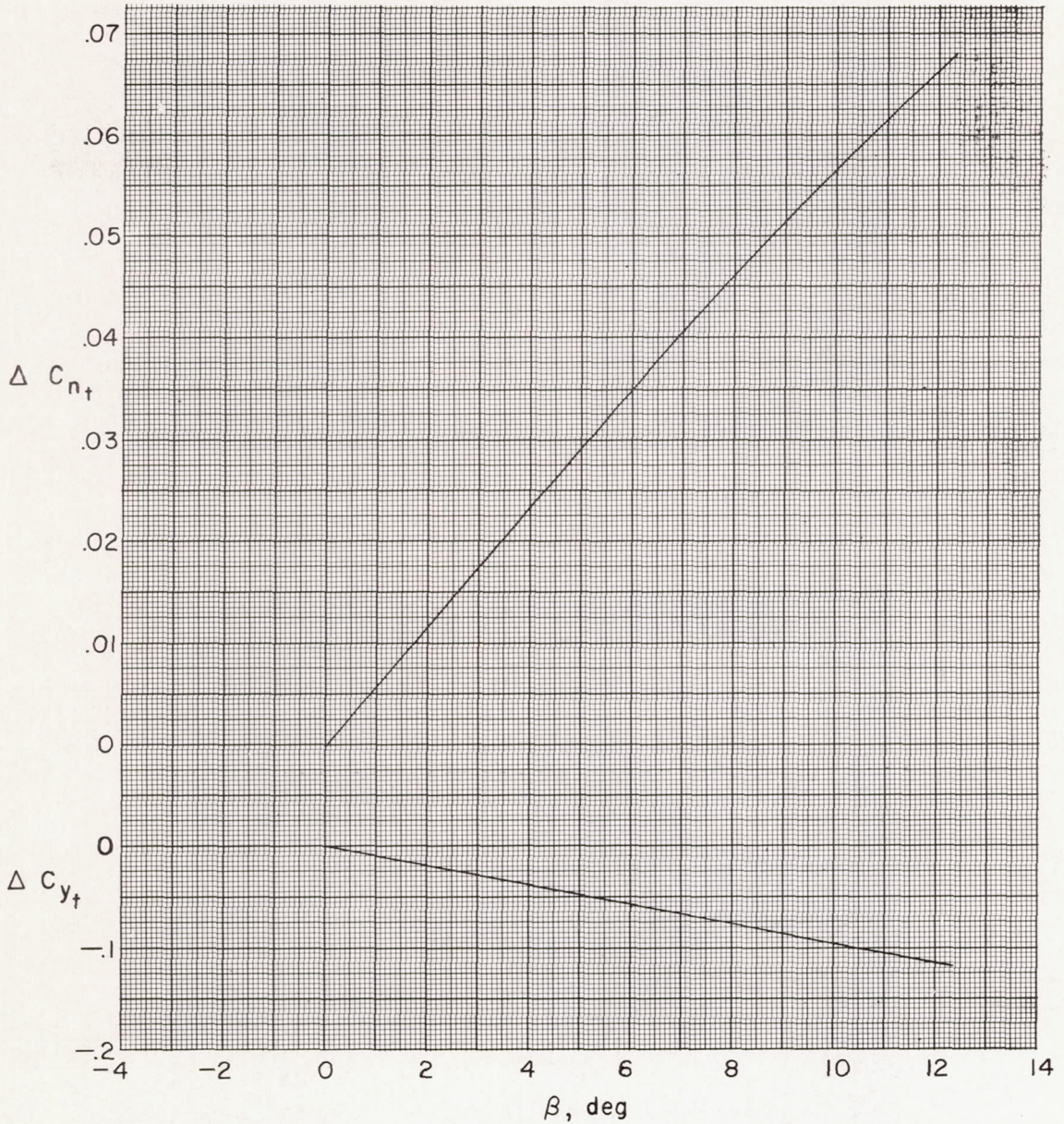
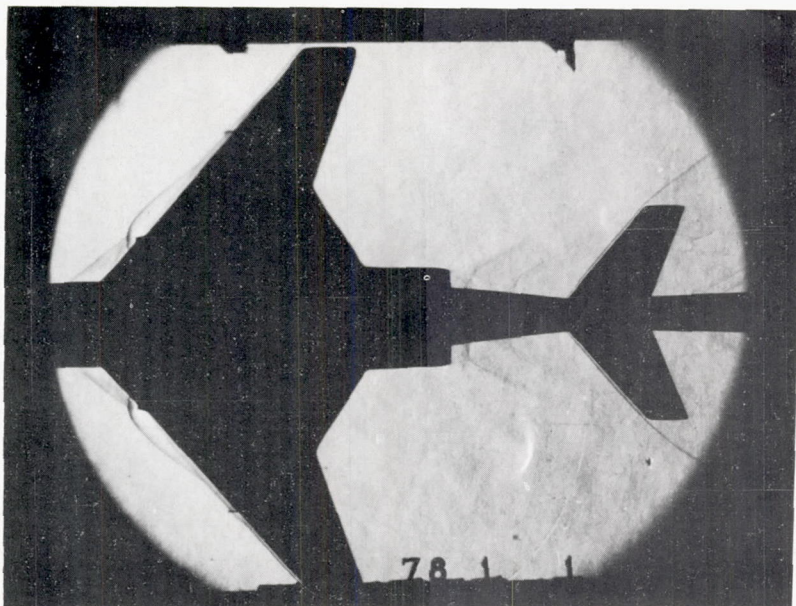
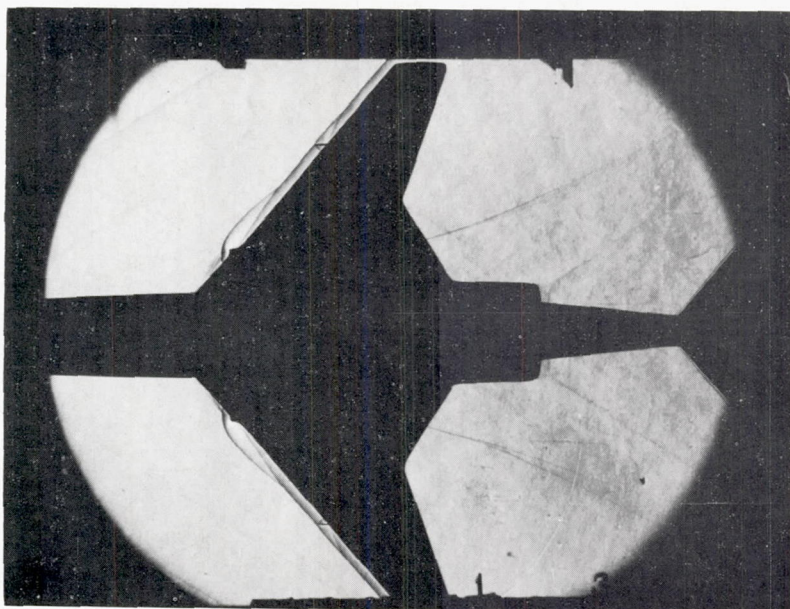


Figure 11.- Incremental lateral-force and yawing-moment coefficients due to the horizontal and vertical tails. $\alpha = -2.2^\circ$; booster adapter off.



$$\alpha = 0^{\circ}; \beta = 0.3^{\circ}$$

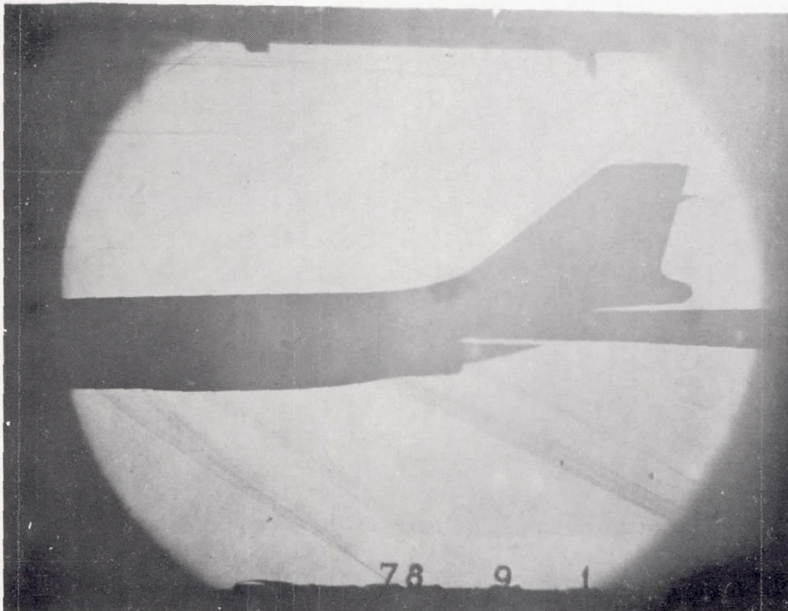
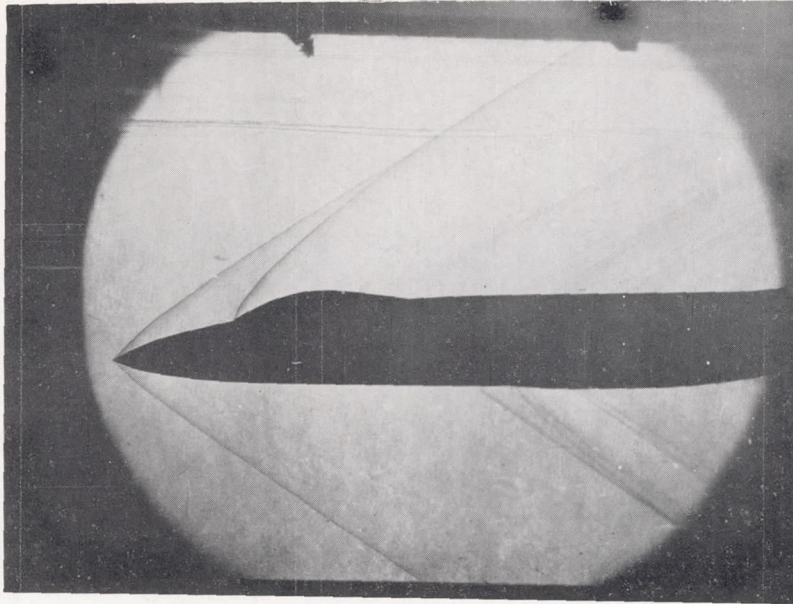


$$\alpha \approx 11^{\circ}; \beta = 0.3^{\circ}$$

(a) Complete model; no adapter.

L-87561

Figure 12.- Schlieren photographs of the various configurations.

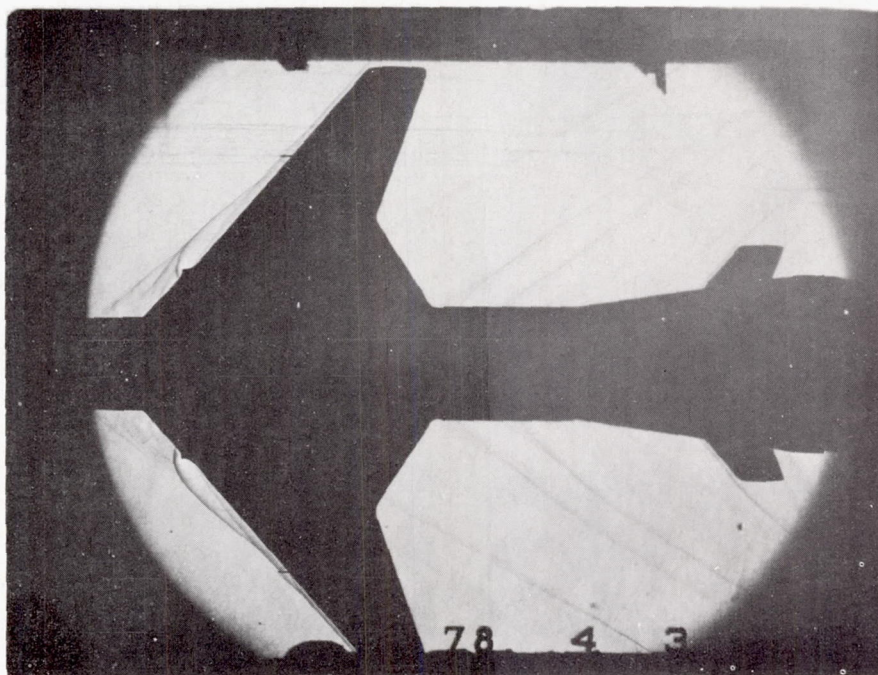


$$\alpha = -2.2^\circ; \beta = 2^\circ$$

(b) Complete model; no adapter.

L-87562

Figure 12.- Continued.

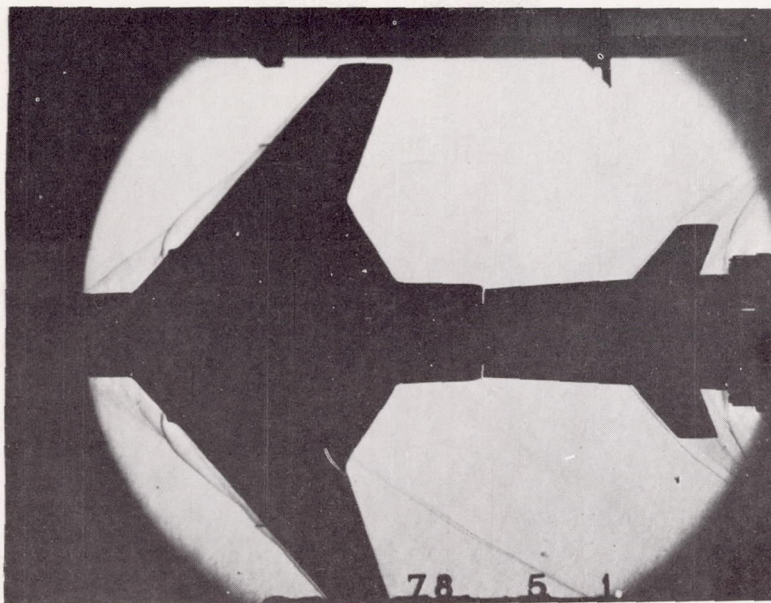


$$\alpha = 0^{\circ}; \beta = 0.3^{\circ}$$

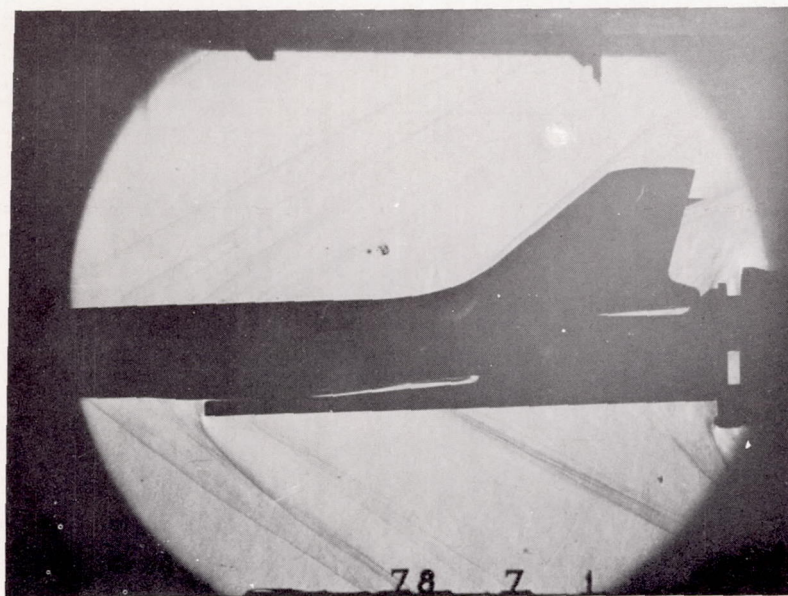
(c) Complete model; original adapter.

L-87563

Figure 12.- Continued.



$$\alpha = 0^\circ; \beta = 0.3^\circ$$

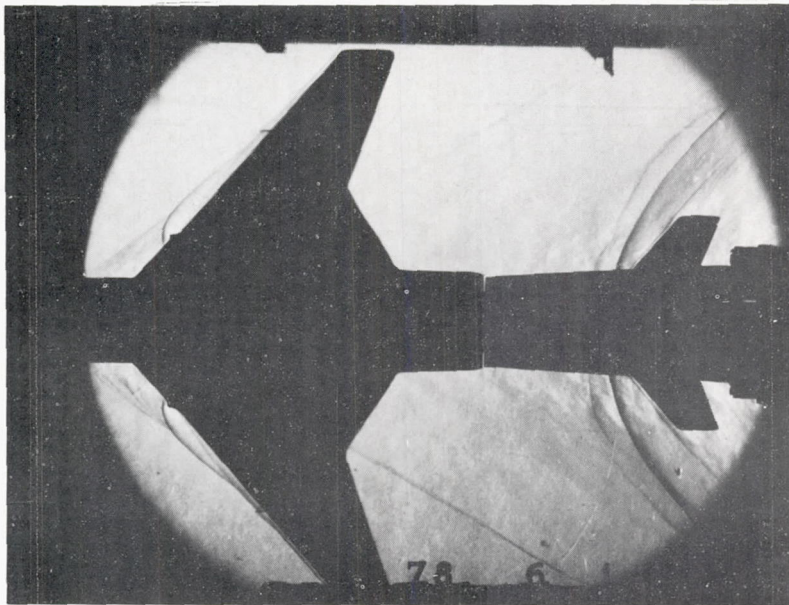


$$\alpha = -2.2^\circ; \beta = 2^\circ$$

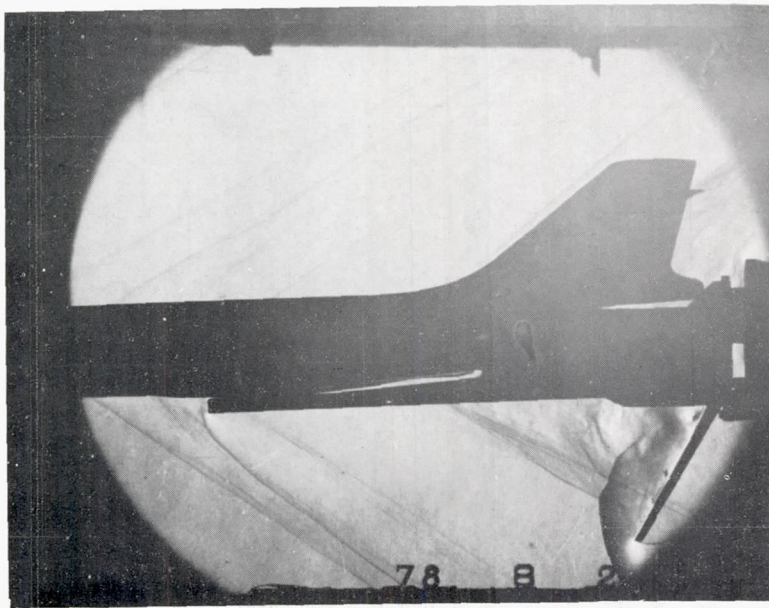
(d) Complete model, revised adapter.

L-87564

Figure 12.- Continued.



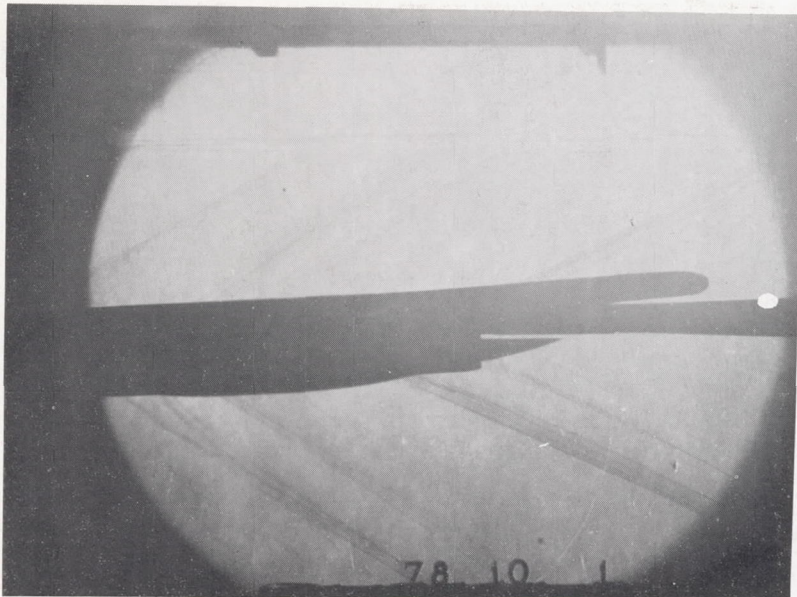
$$\alpha = 0^\circ; \beta = 0.3^\circ$$



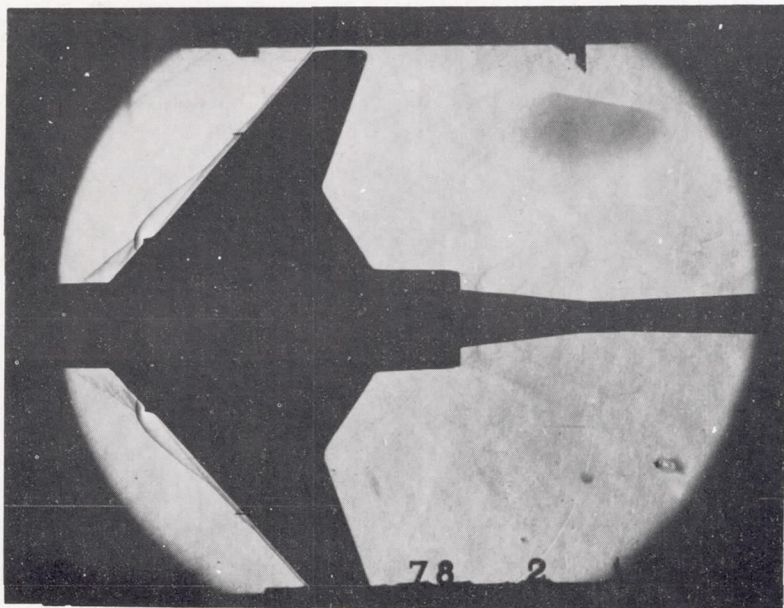
$$\alpha = -2.2^\circ; \beta = 2^\circ$$

(e) Complete model; revised adapter with flap. L-87565

Figure 12.- Continued.



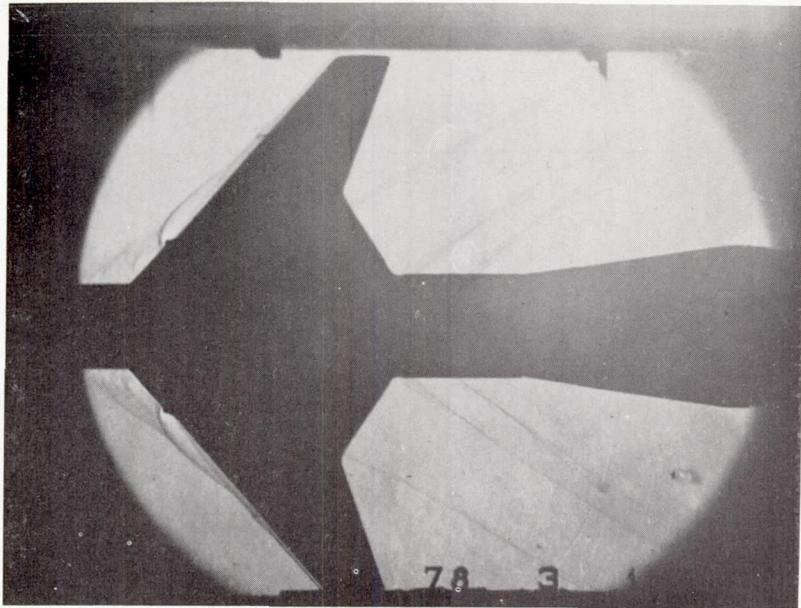
$$\alpha = -2.2^\circ; \beta = 2^\circ$$



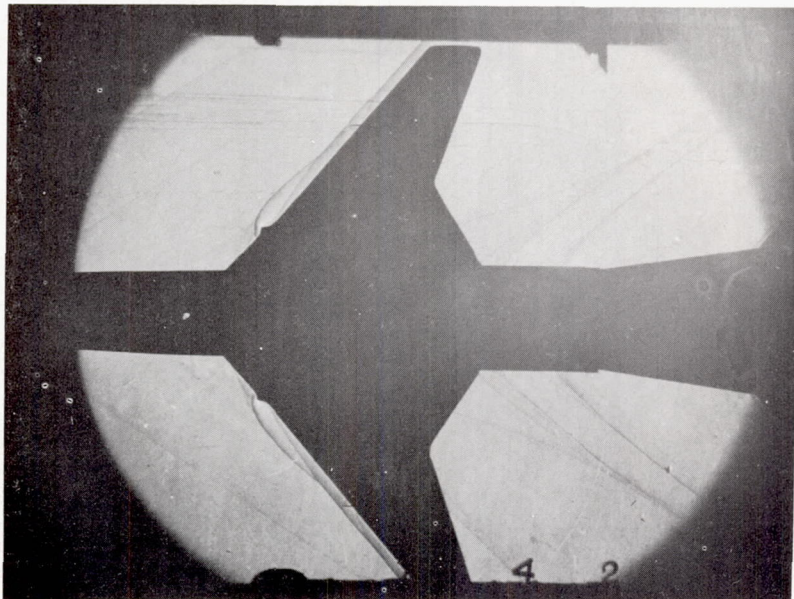
$$\alpha = 0^\circ; \beta = 0.3^\circ$$

(f) Tails off; no adapter. L-87566

Figure 12.- Continued.



$$\alpha = 0^{\circ}; \beta = 0.3^{\circ}$$



$$\alpha = 11^{\circ}; \beta = 0.3^{\circ}$$

(g) Tails off; original adapter.

L-87567

Figure 12.- Concluded.